ORGANIC PROCESS RESEARCH & DEVELOPMENT
OPR&D

pubs.acs.org/OPRD

Article

Development of New Catalytic Asymmetric Routes toward a Cost-Driving Building Block of Nirmatrelvir

Robert Szpera,* Shanjun Huang, Harriet A. M. Fenton, William Waddington, Adam E. S. Gymer, Ian B. Moses, Julia Buck, Heather Ingram, Steven J. Fussell,* Robert Walton, Charles S. Shanahan,* Sarah L. Aleshire, Juliana M. S. Robey, Hanuman P. Kalmode, Michel C. Nuckols, Nageswara R. Kalikinidi, Venumadhav Janganati, Sipak Joyasawal, Chanaka M. Amarasekarage, Chris H. Senanayake, and B. Frank Gupton

Cite This: *Org. Process Res. Dev.* 2024, 28, 2743−2754

Read Online

ACCESS | Metrics & More | Article Recommendations | Supporting Information

ABSTRACT: Nirmatrelvir is an inhibitor of the SARS-CoV-2 main protease and is the active ingredient in Paxlovid. Nirmatrelvir presents a significant synthetic challenge, in no small part due to a cost-driving lactam-containing fragment with two stereogenic centers. Our goal was to help decrease the cost of nirmatrelvir by developing a scalable low-cost synthesis of this fragment, avoiding the use of cryogenic conditions reported in the initial route. Herein, we disclose three catalytic asymmetric routes toward this fragment, via (i) chiral Lewis acid (copper) catalysis, (ii) chiral Brønsted base organocatalysis, and (iii) chiral bifunctional hydrogen-bond-donor organocatalysis.

KEYWORDS: *nirmatrelvir, conjugate addition, copper, Brønsted base, bifunctional hydrogen-bond-donor*

INTRODUCTION

The COVID-19 pandemic created unprecedented levels of mobilization within the scientific community, aimed at developing therapies necessary to address global emergency. To this end, Pfizer developed Paxlovid, which combines ritonavir, a strong CYP3A inhibitor, and nirmatrelvir, an inhibitor of SARS-CoV-2 main protease.[1] Paxlovid was given emergency use authorization for eligible patients by the US FDA in November 2021,[2,3] spurring significant development efforts to make the medication widely available globally. Within this context, Medicines for All Institute at Virginia Commonwealth University (VCU), working with TCG GreenChem Inc. and the Bill & Melinda Gates Foundation, entered into a collaboration with Pfizer to attempt to develop lower-cost processes to produce nirmatrelvir.

The routes reported by Pfizer for preparing nirmatrelvir use fragments **1**, **2**, and **3** (Scheme 1A).[4−9] At the time this research was conducted, the high costs of these starting materials were a contributing factor to the limited global availability of nirmatrelvir and hence also Paxlovid. One particular cost-driver of nirmatrelvir is lactam containing fragment **3**, the synthesis of which is challenging due to the presence of two nonadjacent stereocenters. The established strategy for preparing **3** utilizes a chiral pool approach; *N*-Boc-L-glutamic acid dimethyl ester is doubly deprotonated at −78 °C with excess lithium bis(trimethylsilyl)amide (LiHMDS) and then treated with bromoacetonitrile, resulting in diastereoselective alkylation (Scheme 1B).[10−12] While this method is elegant, it incurs cost in several ways, including the requirement for cryogenic conditions and excess LiHMDS, both of which are expensive on such large scales. Subsequent

Scheme 1. (A) Fragments in Nirmatrelvir Synthesis, (B) Previous Approach to Fragment 3, (C) Asymmetric Catalytic Approach Detailed in This Report

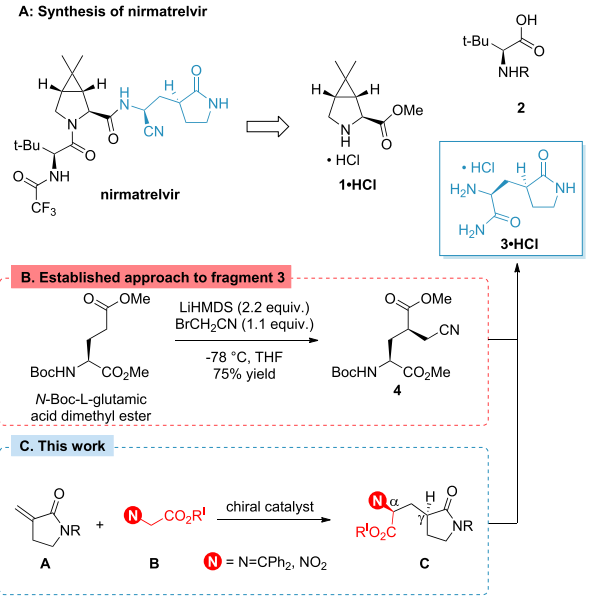

Received: March 15, 2024
Revised: May 10, 2024
Accepted: May 21, 2024
Published: May 28, 2024

reports have studied modifications of this alkylation; however, none have addressed the limitations described above.[13,14] Considering this, development of a noncryogenic and scalable route for the synthesis of **3** is desirable.

An alternate option to the established chiral pool approach described above would be to develop a catalytic asymmetric reaction to prepare fragment **3** or precursors thereof (Scheme 1C). Such approaches may allow one to avoid the use of cryogenic conditions and LiHMDS. In this study, we describe our work to this end. We envisioned setting both α- and γ-stereocenters in a single step via an asymmetric (formal) Michael addition reaction between a lactam containing Michael acceptor **A** and an appropriate pronucleophile **B** (Scheme 1C).[15] The Michael adduct **C** could then be converted into fragment **3** for the synthesis of nirmatrelvir.

RESULTS AND DISCUSSION

Copper Lewis Acid Catalysis. In the Pfizer Sandwich process chemistry laboratories, enantioselective Lewis acid catalysis was considered for setting the α- and γ-stereocenters of the target molecule **3**. There are various reports in the literature of enantioselective Michael additions of glycine imine esters to α,β-unsaturated electrophiles, catalyzed by chiral copper complexes (Scheme 2A). Zajac and co-workers have

Scheme 2. Copper-Catalyzed Asymmetric Michael Addition

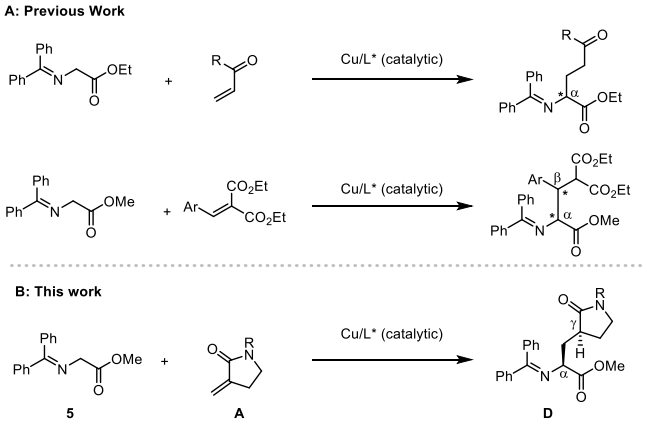

reported Michael addition to enones,[16] Liu, Zhang and co-workers have reported an addition to beta-trifluoromethyl enones,[17] and Arrayás, Carretero, and co-workers have reported an addition to gem-diactivated olefins.[18] Ferrocene-based chiral phosphine ligands were used in each case. In addition to these studies, asymmetric Michael addition of glycine imines has also been reported under Ag(I) and Ca(II) catalysis.[19−22] We anticipated that a similar strategy could be exploited for the enantioselective synthesis of **D** (Scheme 2B). While copper-catalyzed asymmetric Michael addition has been exploited for setting both α- and β-stereocenters, we expected that achieving control of the more remote γ-stereocenter in **D** would be challenging.

Previous reports of copper-mediated Michael additions of glycine imine esters have used relatively activated enones and gem-diactivated alkenes as Michael acceptors.[16−18] We anticipated that the nature of the *N*-substituent of our Michael acceptor would be crucial in rendering it reactive toward **5**. We therefore assessed the reactivity of both NH and *N*-Boc-activated Michael acceptors **6** and **7**. We also assessed reactivity in both the presence and absence of copper to test for undesired background reactivity (Table 1). Reaction mixtures were analyzed by supercritical fluid chromatography−mass spectrometry (SFC-MS) as hydrolysis of the benzophenone imine in both the pro-nucleophile **5** and product **9** was observed under our standard liquid chromatography−mass spectrometry (LC-MS) methods. In addition, chiral SFC enabled the separation of each of the four product stereoisomers for quantification of the reaction stereoselectivity. Our initial experiments were conducted with the achiral ligand 1,1′-bis(diphenylphosphino)ferrocene (DPPF) and 1,8-diazabicyclo[5.4.0]undec-7-ene (DBU) as the base. No product formation or starting material consumption was observed when NH Michael acceptor **6** was used both in the presence and absence of the copper catalyst. In contrast, the more electrophilic *N*-Boc lactam **7** did undergo the desired reaction; 10% SFC area percent (SFC-AP) of a 1:1 mixture of product diastereomers was observed with DBU alone, while in the presence of 1,1′-bis(diphenylphosphino)ferrocene (DPPF) and Cu(I), 97% SFC-AP of a 1.26:1 diastereomeric mixture was obtained in favor of the desired diastereomer. These results suggested that copper could catalyze the reaction and had the potential to control the diastereoselectivity. The observed reaction of **7** with DBU in the absence of copper suggested that screening of different bases would be necessary to avoid background reactivity which would result in reduced ee and DR. Although not tested, it is possible that other substituents in place of *N*-Boc could also activate the Michael acceptor. Glycine imine esters like **5** have also been reported to react in [2 + 3] cycloadditions under copper-catalysis to afford pyrrolidines;[23−25] however, under the conditions tested, we did not detect any formation of such species.

Table 1. Reactivity of NH and NBoc Michael Acceptors under Cu-Catalysis

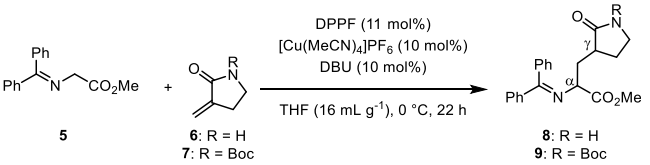

5 | **6**: R = H, **7**: R = Boc | **8**: R = H, **9**: R = Boc

entry	Cu/DPPF	R	base	SFC-AP	DR
1	no	H	DBU	0	NA
2	yes	H	DBU	0	NA
3	no	Boc	DBU	10	1:1
4	yes	Boc	DBU	97	1.26:1

With a proof of concept established using *N*-Boc Michael acceptor **7**, a high-throughput chiral ligand screen was executed to determine whether the reaction could be performed with the desired enantio- and diastereo-selectivity to afford (*S,S*)-**9** (Figure 1).

Literature precedence shows that ferrocene-based phosphine ligands have performed well in copper-catalyzed Michael addition reactions of glycine imine esters,[16−18] so the ligand screen was biased toward ligands of this class; JosiPhos, TaniaPhos, FOXAP, and FesulPhos ligands were all screened. Various bisphosphine ligands were screened, including both those with chiral scaffolds and those chiral at phosphorus. In addition, phorphoramidite, BOX, and PyBox ligands were all screened.

The ligands (R_p)-FesulPhos and (*S,S*)-iPr-FOXAP afforded the highest stereoselectivity for (*S,S*)-**9**; however, the

https://doi.org/10.1021/acs.oprd.4c00109
Org. Process Res. Dev. 2024, 28, 2743−2754

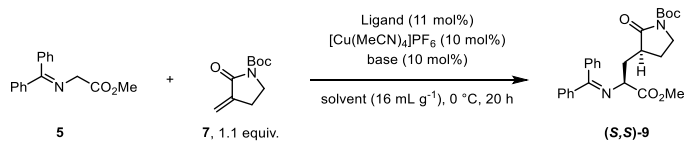

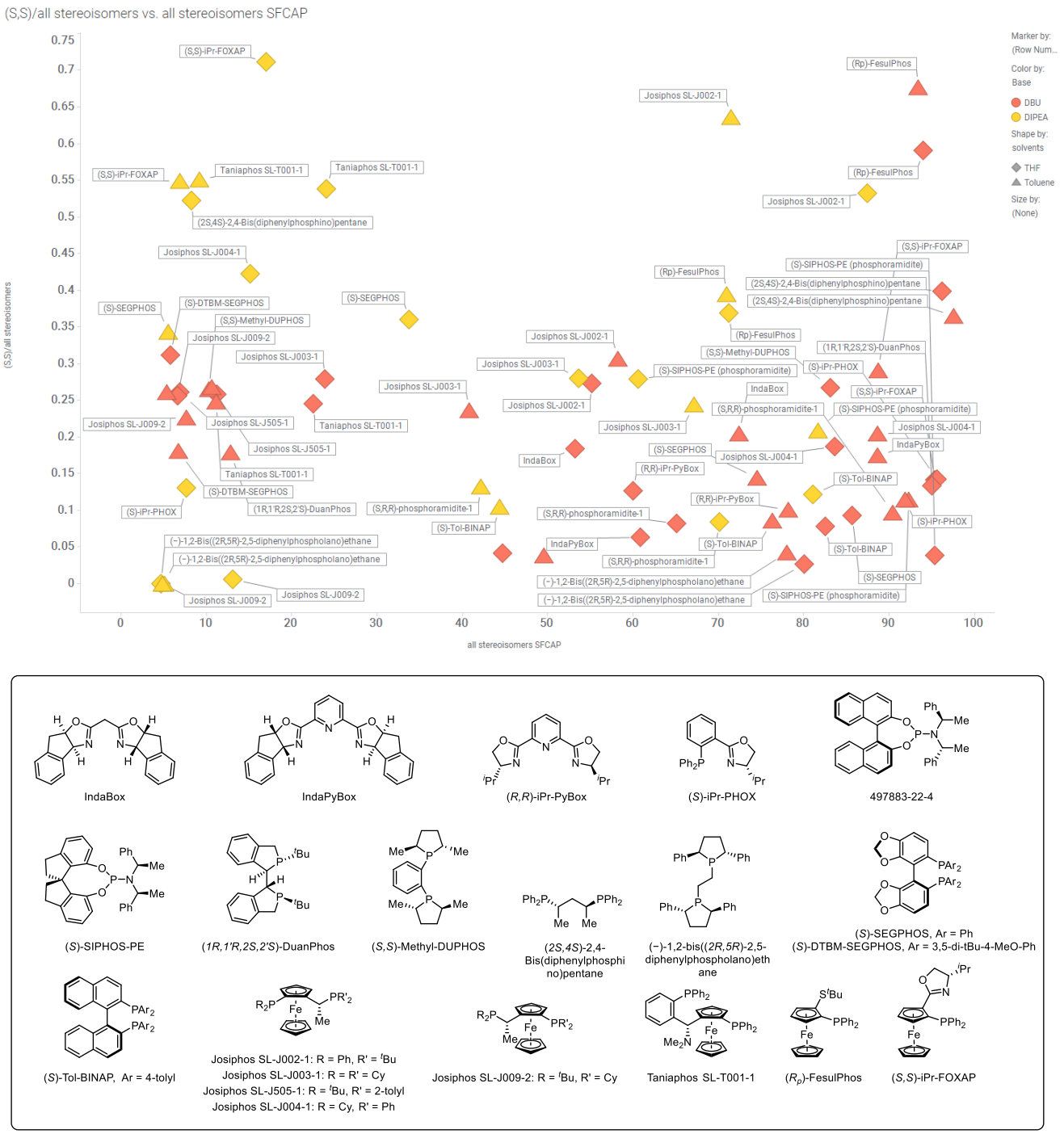

Figure 1. Chiral ligand screen. The SFC-AP of all four product stereoisomers of **9** is plotted on the *x*-axis, and the stereoselectivity is plotted on the *y*-axis, as a fraction of (*S*,*S*)-**9** over all four possible stereoisomers of **9**. The data points are labeled with the ligand used. The shape of the spots corresponds to the solvent used, and the color corresponds to the base. See the legend in the top right of the figure for details.

conversion with (*S*,*S*)-iPr-FOXAP was low. In contrast, the conversion using (R_p)-FesulPhos with DBU was high. A similar analysis was performed for (*R*,*R*)-**9**—if this product stereoisomer was observed with good selectivity, the catalyst enantiomer could be switched to afford the desired product stereoisomer (*S*,*S*)-**9**. Excellent selectivity for (*R*,*R*)-**9** was achieved using (−)-1,2-bis((2*R*,5*R*)-2,5-diphenylphospholano)ethane; however, the conversion was low. Tol-BINAP was slightly less selective but afforded much higher conversion. Nonetheless, (R_p)-FesulPhos performed the

https://doi.org/10.1021/acs.oprd.4c00109
Org. Process Res. Dev. 2024, 28, 2743−2754

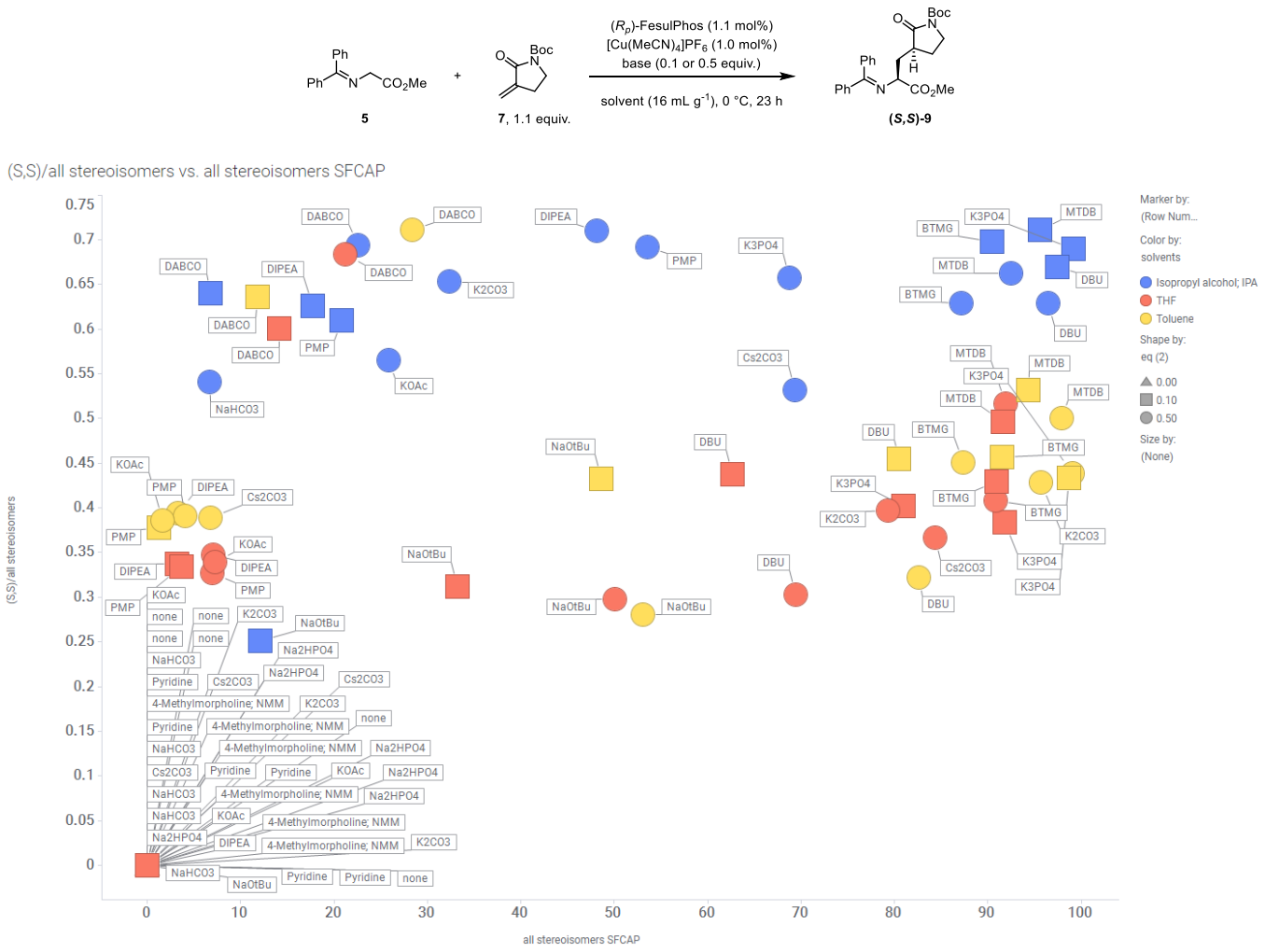

Figure 2. Base and solvent screening at 1 mol % copper loading. The SFC-AP of all four product stereoisomers of **9** is plotted on the *x*-axis, and the stereoselectivity is plotted on the *y*-axis, as a fraction of (*S,S*)-**9** over all four possible stereoisomers of **9**. The data points are labeled with the base used. The shape of the spots corresponds to the equivalents of the base used, and the color corresponds to the reaction solvent. See the legend in the top right of the figure for details.

best overall. Examining the effect of the base, neither DBU nor DIPEA was preferred outright, with the best base being dependent on the ligand used. The desired (*S,S*)-**9** stereoisomer was assigned by comparison of SFC retention time with an independently prepared sample (see the Supporting Information for full details).

In preparation for the reaction scale-up, we aimed to develop conditions with a lower catalyst loading. Using (R_p)-FesulPhos as the ligand with 1 mol % copper loading, a range of bases were tested at both 0.5 and 0.1 equiv, in addition to a small selection of solvents (Figure 2). Multiple of the conditions tested resulted in the formation of the product with conversions and stereoselectivity similar to that observed employing 10 mol % of catalyst. Organic bases of various strengths were competent in the reaction, including DBU, 7-methyl-1,5,7-triazabicyclo[4.4.0]dec-5-ene (MTDB), and 2-*tert*-butyl-1,1,3,3-tetramethylguanidine (BTMG) and tertiary amines *N,N*-diisopropylethylamine (DIPEA), pentamethylpiperidine (PMP), and 1,4-diazabicyclo[2.2.2]octane (DABCO). In contrast, the weaker organic bases *N*-methyl-morpholine (NMM) and pyridine resulted in no conversion. Inorganic base K_3PO_4 was also competent and to a lesser extent K_2CO_3. Weaker bases $NaHCO_3$, Na_2HPO_4, and KOAc were ineffective, resulting in very low or zero conversion. The use of NaOtBu resulted in the significant formation of side products. The reaction did not proceed in the absence of a base.

In general, isopropyl alcohol (IPA) resulted in significantly higher selectivity for desired (*S,S*)-**9** than either toluene or tetrahydrofuran (THF). This was primarily due to the higher diastereomeric ratios (DRs) with IPA, but enantiomeric excesses (ees) were also higher. Whether 0.1 or 0.5 base equivalents performed better was dependent on the base strength; for DIPEA, DABCO, and PMP, 0.5 equiv performed better due to increased conversion and higher DR. For stronger bases MTDB, DBU, BTMG, and K_3PO_4, 0.1 equiv was favored due to higher ee and DR and reduced impurity formation. Overall, reactions with DIPEA (0.5 equiv), MTDB (0.1 equiv), and BTMG (0.1 equiv) in IPA and DABCO (0.5 equiv in toluene) afforded the greatest stereoselectivity for the desired product. While MTDB and BTMG afforded higher conversions, DIPEA was selected for continued optimization due to its lower cost.

It was suspected that increasing the DIPEA equivalents beyond 0.5 would increase the conversion based on results with 0.1 and 0.5 equiv shown in Figure 2. Screening of various

https://doi.org/10.1021/acs.oprd.4c00109
Org. Process Res. Dev. 2024, 28, 2743−2754

DIPEA equivalents was therefore carried out (Table 2). Increasing above 0.5 equiv further increased the conversion

Table 2. Optimization of DIPEA Equivalents

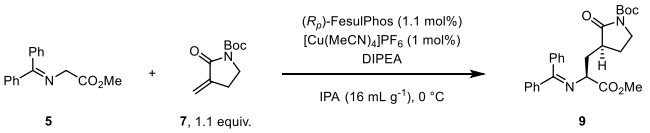

entry	DIPEA equiv.	SFC-AP	%ee (*S*,*S*)	DR	(*S*,*S*)/(all stereoisomer)
1	0.25	36	97.3	2.12:1	0.670
2	0.50	54	97.2	2.40:1	0.696
3	1.0	72	97.6	2.71:1	0.722
4	2.0	79	97.8	2.91:1	0.736
5	2.5	86	97.8	2.94:1	0.738
6	3.0	88	97.9	3.00:1	0.742
7	3.5	84	97.8	3.05:1	0.745

and DR of the reaction while maintaining a high ee of over 97%. The beneficial effect of increased DIPEA plateaued at around 2.5 equiv.

Due to the pronounced effect of solvent observed in the base/solvent screening in Figure 2, a further selection of solvents was tested (Table 3). Protic solvents (entries 1−4)

Table 3. Further Solvent Screening

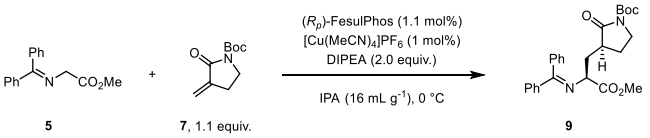

entry	solvent	SFC-AP	%ee (*S*,*S*)	DR	SS/(all stereoisomer)
1	IPA	79	97.8	2.91:1	0.736
2	MeOH	82	92.7	0.93:1	0.465
3	EtOH	91	95.7	0.85:1	0.449
4	tAmOH	51	97.9	2.56:1	0.712
5	THF	13	79.4	0.71:1	0.372
6	toluene	8	85.3	0.82:1	0.418
7	heptane	9	80.8	0.62:1	0.347
8	EtOAc	9	82.1	0.67:1	0.365

afforded significantly higher conversions than all other solvents tested, which resulted in only very poor conversions. The nature of the alcohol had a large effect on the diastereoselectivity; both IPA and tAmOH favored the formation of the desired diastereomer, while MeOH and EtOH resulted in near-equal quantities of both diastereomers. Nonetheless, with all protic solvents, the ee values remained above 90%. Similar optimization of the base equivalents and solvent was also carried out using DBU as a base; however, the results were inferior to those obtained using DIPEA.

Which of the two stereocenters of **9** is set with a high level of control (>97% ee) and which with less control (∼3:1 DR) was not determined; however, based on prior literature, we believe that it is likely that it is the center α to the ester that is set with high control.[16]

Next, the kinetics of the reaction were investigated under different copper catalyst loadings (Figure 3). Automated reaction mixture sampling was performed using an Unchained Laboratories CM3. In this manner, concentration versus time profiles for four separate reactions could be acquired

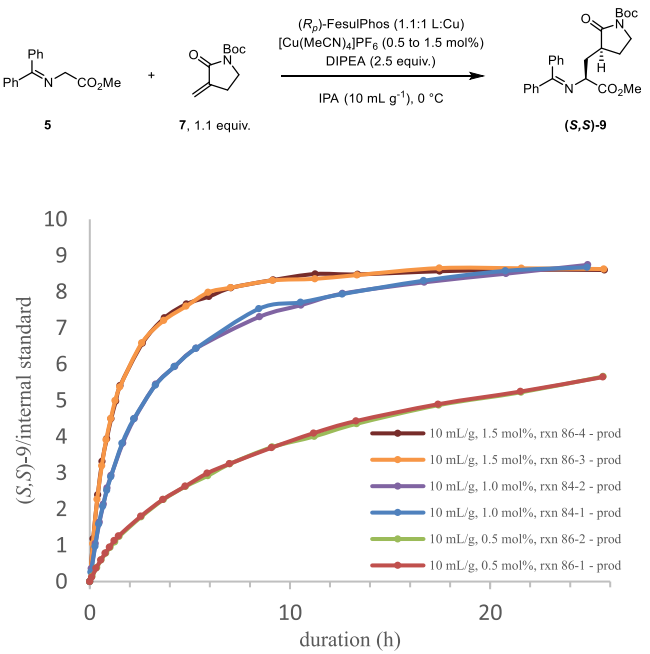

Figure 3. Time-course data for varying catalyst loadings.

simultaneously and autonomously. Excellent reproducibility in kinetic data was seen between repeats of the same reaction conditions, as shown in Figure 3. These time-course experiments were conducted at 10 mL g^{-1} rather than 16 mL g^{-1}, which resulted in a faster reaction. Reducing the catalyst loading to 0.5 mol % resulted in a slower reaction, with a significant starting material remaining after 24 h. Contrarily, increasing the loading to 1.5 mol % resulted in the reaction reaching completion in roughly 10 h instead of 20. An increase in DR was also observed as catalyst loading was increased, with 1.5 mol % copper giving ∼3.35:1 selectivity for the desired diastereomer. The ee remained approximately unchanged with different catalyst loadings. Throughout the reactions, both the ee and the DR of the product remain approximately constant. It is likely that increasing the concentration further would result in shorter reaction durations. The purity of the Michael acceptor **7** was also found to impact the reaction rate, with less pure batches reacting more slowly and resulting in lower product DR. We speculated that the lower rate may be due to impurities binding to copper, thus inhibiting catalysis.

The optimization experiments discussed hereto were conducted in a nitrogen-filled glovebox with ∼12 mg of **5** in 1 mL vials with magnetic stirring (time-course experiments in 4 mL vials with ∼126 mg of **5**). To demonstrate the practicality and scalability of the chemistry, we sought to demonstrate the reaction in a manner relevant to process chemistry−outside of the glovebox with overhead stirring on a multigram scale. Prior to scaling the reaction, process safety testing was carried out (see Supporting Information for further information). Differential scanning calorimetry (DSC) analysis of **7** showed an early endotherm from 59 °C, attributed to the compound melting, immediately followed by an exotherm at −280 J g^{-1}, indicating a medium severity event.[26] This prompted further work to understand the reaction safety limits in more detail. DSC experiments performed on **5** and **9** showed some low thermal onsets between −50 and −100 J g^{-1}, indicating low-severity thermal events.[26] Further thermal stability assessment of the reaction mixture was conducted

https://doi.org/10.1021/acs.oprd.4c00109
Org. Process Res. Dev. 2024, 28, 2743−2754

via a thermal screening unit (TSU), with no significant thermal onsets observed up to 248 °C, with gas observed from 150 °C attributed to thermal loss of the Boc-protecting group. This analysis demonstrated that the intended conditions were safe for further scale-up.

Scale-up reactions were performed outside the glovebox on a bench in an EasyMax reactor equipped with overhead stirring. Initial 1 g reactions resulted in SFC profiles very similar to those observed in small-scale optimization studies. The ease of scale-up is likely in part due to the homogeneity of the reaction mixture. From a 1 g experiment, product **9** was isolated via flash chromatography, in an isolated yield of 77% as a mixture of stereoisomers (3.93:1 DR, 99.0% ee). Due to the propensity of **9** to undergo hydrolysis, we sought to develop a telescoped procedure to isolate the deprotected product as the (−)-camphorsulfonic acid ((−)-CSA) salt **10·(−)-CSA**. However, DIPEA carried through from the copper-catalyzed reaction resulted in difficulties isolating pure **10·(−)-CSA**, as the product was contaminated with DIPEA salts. We therefore investigated methods to remove DIPEA prior to deprotection/salt formation. Attempted precipitation of DIPEA from the reaction mixture as a salt using anhydrous HCl, $NaHSO_4.H_2O$, and TFA led to the undesired cleavage of the benzophenone imine. Instead, the removal of DIPEA was achieved by passing the reaction mixture through a silica plug. Subsequent solvent swap into TBME and heating with (−)-CSA, followed by the addition of acetone, afforded the product as a free-flowing solid. Using this process, a 5 g scale reaction-deprotection-resolution was conducted, resulting in a 67% isolated yield of (*S,S*)-**10·(−)-CSA** (Scheme 3). Analysis of crude intermediate

Scheme 3. Scale-Up of Synthesis of (*S,S*)-10·(−)-CSA Using Asymmetric Copper Catalysis

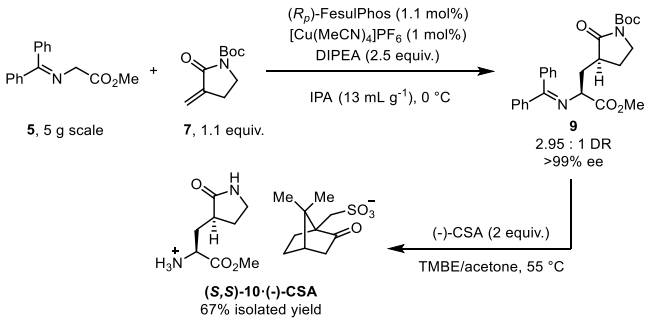

9 by SFC showed a DR of 2.95:1 and an ee >99%. The reduced DR of **9** in this run relative to other gram-scale experiments was likely due to use of a slightly less pure batch **7**; the use of a purer batch of **7** would likely result in a higher DR of **9** and thus a higher isolated yield of (*S,S*)-**10·(−)-CSA**. The use of (−)-CSA for the deprotection and salt formation enabled the isolation of the product as a single diastereomer. Salts of **10** can be easily converted into nirmatrelvir fragment **3** via $MgSO_4$-mediated aminolysis.[8]

Chiral Brønsted Base Catalysis. While Pfizer Sandwich focused efforts on copper catalysis, the Medicines for All Institute investigated leveraging chiral Brønsted base catalysis to control asymmetric Michael addition. The Lambert group has previously reported that chiral cyclopropeninime Brønsted bases such as **11** can catalyze the asymmetric Michael addition of glycine imines with various Michael acceptors (Scheme 4).[27,28] No examples of α,β-unsaturated amides, or amides as Michael acceptors were reported.

Scheme 4. Chiral Brønsted Base-Catalyzed Michael Addition

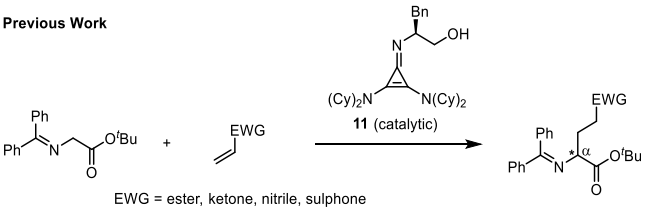

Investigation by the Medicines for All Institute began by exploring the use of the chiral catalyst **11** for controlling asymmetric Michael addition between **5** and **7** (Table 4).[27,28]

Table 4. Solvent Screen Using Chiral Brønsted Base Catalyst 11

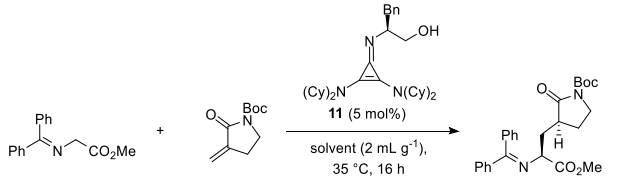

entry	solvent	7 at 16 h (LC-AP)	DR	%ee (*S,S*)
1	TBME	4.1	7.33:1	86
2	CH_2Cl_2	6.0	2.23:1	ND
3	EtOAc	10	2.13:1	ND
4	2-MeTHF	4.0	1.94:1	ND
5	toluene	3.0	4.88:1	84

These experiments were immediately fruitful and provided the desired product in good conversion and enantioselectivity with selectivity for the desired diastereoisomer. Consistent with the observations of the Pfizer Sandwich team, reverse-phase HPLC methods rapidly hydrolyzed the benzophenone imine in **5** and product **9**. The primary amine hydrolyzed product (**19**, Scheme 8) was therefore used to quantify reaction diastereoselectivity via LC−MS. Additional minor peaks were also observed by LC−MS, which were speculated to arise through the rearrangement of the deprotected amine (**20**, Scheme 8). This made quantifying conversion difficult, and thus, for optimization studies, the consumption of **7** was tracked to assess conversion. Later, an SFC method was developed for quantifying the enantiomeric excess of compound **9** directly. Initial screening showed that various solvents resulted in a high conversion of **7**; however, *tert*-butyl methyl ether (TBME) was favored based on the high diastereoselectivity afforded. Good ee was also obtained using TBME. Toluene performed comparably, albeit with slightly lower diastereoselectivity. It should be noted that weaker chiral bases such as $(DHQ)_2Pyr$ were also tested and did indeed form the desired adduct, however with low stereocontrol.

We next sought to improve the cost-effectiveness of the reaction by attempting to lower the catalyst loading (Table 5). Consumption of Michael acceptor **7** was monitored at 2 and 16 h of reaction time. This analysis showed that the majority of the conversion was complete within 2 h. At higher loadings of

https://doi.org/10.1021/acs.oprd.4c00109
Org. Process Res. Dev. 2024, 28, 2743−2754

Table 5. Effect of Loading of Catalyst 11 on Conversion of 7 and DR

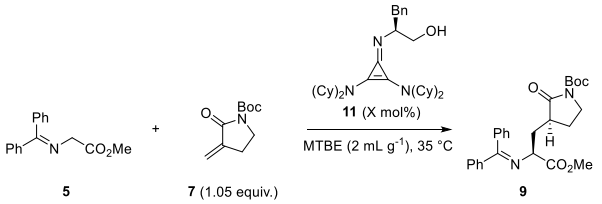

entry	11 (mol %)	7 (LC-AP, 2 h)	7 (LC-AP, 16 h)	DR (16 h)
1	10	4.5	3.5	6.87:1
2	5	4.7	4.1	7.33:1
3	4	4.4	3.0	6.87:1
4	3	7.0	5.5	6.81:1
5	2	9.3	6.6	6.75:1
6	1	13.6	12.2	6.41:1
7	5 (5g scale)	n/a	2.7	6.69:1

catalyst **11**, we observed similar results when tracking consumption of **7**, but the conversions slightly decreased at 3 mol % and below. Reducing the catalyst loading had a minimal effect on the DR of the reaction. Performing the reaction on a 5 g scale with a 5 mol % catalyst, only 3% LC-AP of **7**, which was used in excess, remained after 16 h. Under conditions that afforded incomplete conversion at 16 h, the reactions appeared to be stalling, as minimal further conversion was observed at later time points.

In order to achieve full conversion with lower catalyst loading, we next explored reaction temperature and concentration effects (Table 6). Increasing the reaction temperature from 35 to 55 °C while using 2 mol % of **11** resulted in almost complete conversion being observed at 2 h; however, a reduced DR of 4.29:1 was observed, compared to 6.81:1 at 35 °C. At 1 mol % catalyst loading at 35 °C, conversion was incomplete after 16 h; however, by increasing the concentration to 3 mL g^{-1} and increasing the temperature to 40−45 °C, complete conversion was achieved with a less severe reduction in DR (5.80:1).

The scalability of this chemistry was demonstrated using 7 g of **5** and 2 mol % of catalyst **11**, followed by a telescoped deprotection/resolution to afford **(*S*,*S*)-10·(−)-CSA** in 66% yield (Scheme 5).

Bifunctional Hydrogen-Bond-Donor Catalysis. In addition to Brønsted base catalysis, the Medicines for All Institute also investigated asymmetric bifunctional hydrogen-bond-donor (HBD) catalysts. These catalysts have been shown to be competent in controlling the stereochemistry of Michael additions with nitroalkane pro-nucleophiles.[29] Control over both α- and β-stereocenters (relative to the nitro group) in Michael adducts has been demonstrated, however without stereocontrol at the γ-position (Scheme 6A).[30] Nitroacetate pro-nucleophiles have also been used in Michael additions under bifunctional HBD catalysis; however, achieving control at the α-stereocenter with such nucleophiles is difficult, presumably due to epimerization at the acidic α-carbon (Scheme 6B).[31] We, therefore, anticipate that controlling both the α- and γ-positions with a nitroacetate pro-nucleophile could be challenging, but that after nitroacetate reduction,

Scheme 5. Scale-Up of Synthesis of (*S*,*S*)-10·(−)-CSA Using Asymmetric Brønsted Base Catalysis

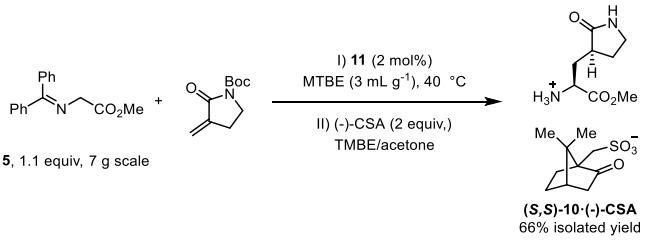

Scheme 6. Bifunctional Hydrogen-Bond-Donor-Catalyzed Michael Addition of Nitro Compounds

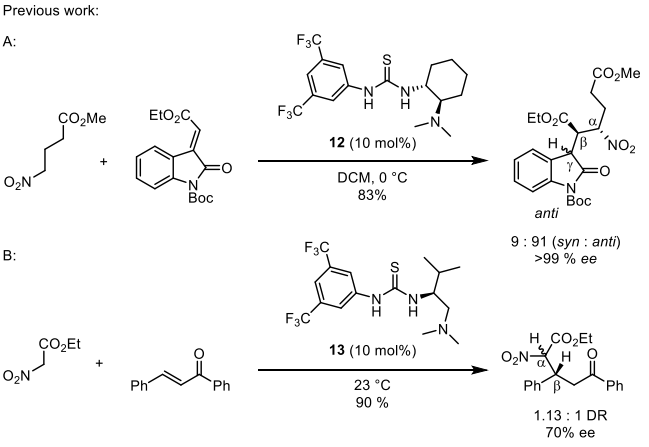

Table 6. Effect of Catalyst Loading, Concentration, and Reaction Temperature on Conversion of 7 and DR

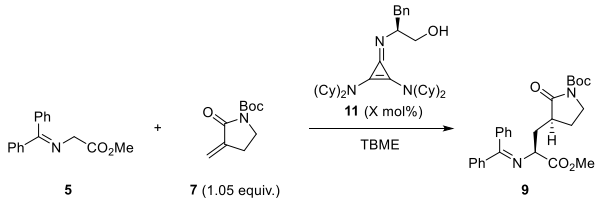

entry	11 (mol %)	conc (ml g^{-1})	temp (° C)	7 (LC-AP, 2 h)	7 (LC-AP, 16 h)	DR (16 h)
1	2	5	35	9.3	6.6	6.81:1
2	2	5	55−60	3.5	3.2	4.29:1
3	2	2	55−60	3.5	2.8	4.15:1
4	1	5	35	13.6	12.2	n/a
5	1	5	55−60	12.0	11.0	n/a
6	1	3	40−45	4.6	3.7	5.80:1

https://doi.org/10.1021/acs.oprd.4c00109
Org. Process Res. Dev. 2024, 28, 2743−2754

Table 7. Optimization of Asymmetric Bifunction HBD-Catalyzed Michael Addition of Nitroacetates into 7[a]

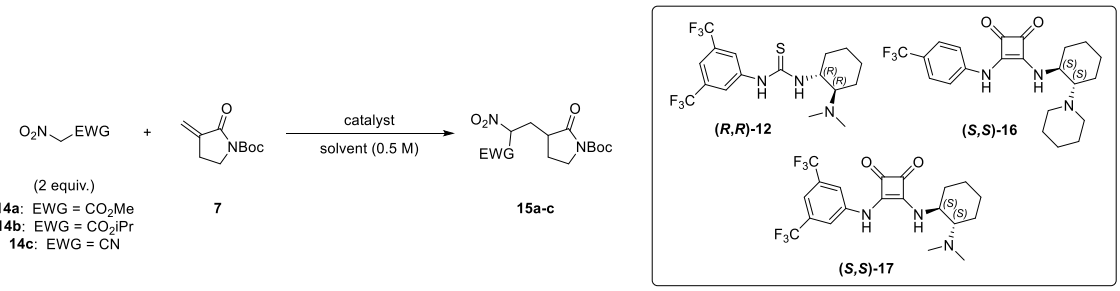

entry	EWG	catalyst (mol %)	solvent	temp (°C)	time	DR	%ee (*S*,*S*)
1	CO_2Me[b]	NEt_3	DCM	rt	2 h	1.22:1	0
2	CO_2Me	(*R*,*R*)-**12** (10)	DCM	rt	6 h	1.27:1	−69
3	CO_2Me	(*R*,*R*)-**12** (10)	toluene	rt	6 h	1.38:1	−66
4	CO_2Me	(*S*,*S*)-**16** (10)	DCM	rt	6 h	1.33:1	36
5	CO_2Me	(*S*,*S*)-**17** (10)	DCM	rt	2 h	1.22:1	89
6	CO_2Me	(*S*,*S*)-**17** (10)	2-MeTHF	rt	30 min	1:1	89
7	CO_2Me	(*S*,*S*)-**17** (10)	2-MeTHF	40 °C	1.5 h	1.22:1	90
8	CO_2Me	(*S*,*S*)-**17** (1)	2-MeTHF	40 °C	24 h	1.17:1	88
9[c]	CO_2Me	(*S*,*S*)-**17** (1)	2-MeTHF	40 °C	24 h	1.22:1	85
10[d]	CO_2Me	(*S*,*S*)-**17** (1)	2-MeTHF	40 °C	24 h	1.17:1	86
11	$CO_2{}^{i}Pr$	(*S*,*S*)-**17** (1)	2-MeTHF	40 °C	24 h	1.33:1	83
12	CN	(*S*,*S*)-**17** (1)	2-MeTHF	40 °C	24 h	ND[e]	

[a]Unless otherwise stated, each reaction in the above table proceeded with complete conversion of 7 by NMR. [b]Using 5 equiv of methyl nitroacetate. [c]Reaction run with 1.3 equiv of methyl nitroacetate, complete conversion of 7 by NMR, 95% isolated yield of the stereoisomeric mixture was obtained after workup and column purification. [d]Reaction run with 1.1 equiv of methyl nitroacetate showed >95% conversion of SM to product but did show some remaining SM after 24 h. [e]Reaction with nitrile showed very little conversion to product.

separation of the less configurationally labile amino ester diastereomers would provide access to the core structure of fragment **3**.

We started our investigation by testing various catalysts in the reaction between Michael acceptor **7** and methyl nitroacetate **14a** (Table 7).[1] The nonenantioselective reaction was carried out by the action of triethylamine alone, providing adduct **15a** with full conversion (by quantitative NMR) to give a nearly 1:1 mixture of diastereomers (entry 1). We then turned our attention to bifunctional HBD catalysts (**12**, **16**, and **17**). Utilizing the chiral thiourea catalyst (***R*,*R*)-12** (at 10 mol %), we observed rapid reactivity under ambient conditions to provide **15a** with full conversion (qNMR) in −69% ee as a near equal mixture of diastereomers (entry 2). While we did not definitively assign which of the two stereocenters is controlled in the reaction, we suspect it to be that in the pyrrolidinone ring, as that α to the nitro group is likely to be highly labile. We then evaluated the squaramide-based catalyst (***S*,*S*)-16**, which afforded a reduced ee of 36% (entry 4). However, the more reactive chiral squaramide (***S*,*S*)-17**, featuring the same 3,5-bis(trifluoromethyl)aniline moiety as **12**, afforded both excellent reactivity and enantioselectivity, providing **15a** with full conversion in 2 h in 89% ee and 55:45 DR (entry 5).

Further optimization was conducted with (***S*,*S*)-17** due to its higher enantioselectivity and reactivity (shorter duration to reach reaction completion). We next looked at the effect of solvent and found that 2-MeTHF gave superior reactivity, with complete consumption of **7** observed within 30 min, while maintaining high enantioselectivity (Table 2, entry 6). Reducing catalyst loadings, however, greatly increased the time required for the reaction to reach completion, from 30 min at 10 mol % to over 24 h at 1 mol % when running the reaction at room temperature. We then found that increasing the reaction temperature to 40 °C was sufficient for completing the reaction within 24 h using 1 mol % of catalyst, providing **15a** in 1.17:1 DR and 88% ee (entry 8).

In attempts to reduce the cost of this reaction further, we evaluated lowering the equivalent of methyl nitroacetate **14a** (entries 9 and 10). We found that 1.3 equiv was still sufficient to drive the reaction to completion; however, 1.1 equiv resulted in detectable amounts of **7** remaining after 24 h. In an attempt to improve the DR, we tested use of the bulkier *i*-propyl nitroacetate **14b**; however, the change in DR was negligible (entry 11). This is likely due to epimerization at the acidic α position.

Next, we briefly looked at nitroacetonitrile **14c** as an alternative activated nitromethylene nucleophile that could be similarly used to access the key starting material **3** (entry 12). However, we found that the reaction provided a very low conversion to the product, and thus, we did not explore this further. Given the superior reactivity and commercial availability of methyl nitroacetate as the nucleophile, we opted to advance **14a** in our synthesis of **3**.

We next turned our attention to scaling up and further optimizing the reaction of methyl nitroacetate **14a** and Michael acceptor **7**. Process safety testing of methyl nitroacetate highlighted some of the thermal stability concerns. DSC showed an exotherm from 161 °C at −2291 J g^{-1}, indicating a high severity event[26] which is common for nitro-based compounds.[32] Six trials were conducted using the BAM Falhammer test apparatus with an impact energy of 60 J, showing no reaction overall, indicating that the compound is unlikely to be shock-sensitive.

For scale-up experiments, we aimed to drive down the catalyst loading as much as possible as the catalyst was a

https://doi.org/10.1021/acs.oprd.4c00109
Org. Process Res. Dev. 2024, 28, 2743−2754

significant cost driver. At a 25 g scale, we used 0.5 mol % of (*S,S*)-**17** and observed noticeably slower reaction rates. At 1.3 equiv of methyl nitroacetate, not only was the reaction slower but the bis-alkylated side product **18** was also found to be a significant contributor to the final reaction profile (>10% of the mixture by LC-AP). When 2 equiv of methyl nitroacetate was used in a 25 g scale reaction, the progress was faster and the side product was observed in reduced quantities (<5% by LC-AP, Scheme 7). We also found that performing the reaction at reflux facilitated reaction progression at low catalyst loading; however, a reduction in ee to 76% was observed.

Scheme 7. Optimized Scale-Up of Asymmetric Michael Addition of Methyl Nitroacetate and 7

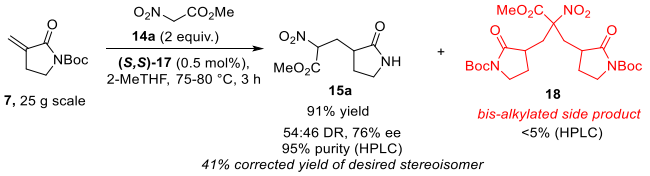

With sufficient quantities of **15a** in hand, we turned our attention to advancing toward key starting material **3** (Scheme 8). We first reduced the nitro group by hydrogenation but

Scheme 8. Advancement of Michael Adduct 15a to (*S,S*)-10·(−)-CSA

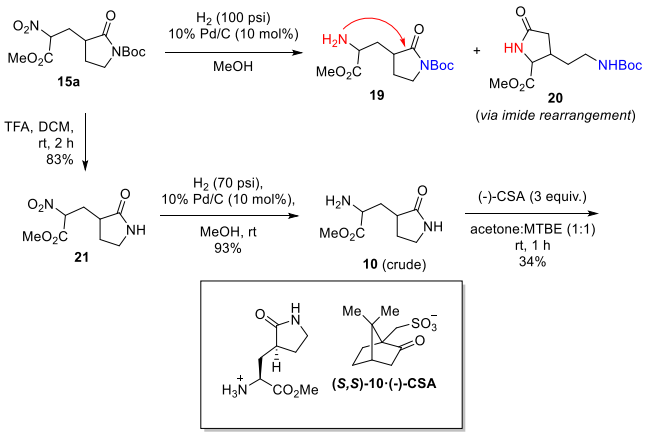

quickly found that the liberated free amine **19** undergoes facile rearrangement by reaction with the imide carbonyl to give lactam **20**. In order to suppress this reaction, the Boc group of **15a** needs to be removed first to afford the less electrophilic lactam **21**, which can be prepared in 83% yield by treatment with TFA, followed by purification by simple precipitation. Next, the nitro group of compound **21** was reduced by hydrogenation. In this case, no rearrangement product was observed, furnishing product **10** in a 93% yield. Crude **10** was advanced to the resolution step without further purification, and treatment with (−)-CSA provided (*S,S*)-**10**·(−)-**CSA** in a 34% isolated yield after recrystallization.

Comparison of Approaches and Conclusions. Over the course of exploring the various asymmetric approaches described, a few significant advantages of using the methyl glycine imine **5** chemistry over using the methyl nitroacetate **14a** chemistry became apparent; (i) **5** is lower in cost and available in greater supply than **14a**, (ii) **5** has a more favorable safety profile than **14a** based on DSC analysis and (iii) adduct **9** derived from **5** is already in the correct oxidation state to advance toward **3**, unlike the adduct derived from nitroacetate **14a**. In addition, although enantioselectivity could be controlled using **14a**, no control of diastereoselectivity was observed under the conditions investigated. This is likely due to the configurational lability of carbon α to the nitro group in adducts derived from **14a**. In contrast, the reaction of **7** under both copper catalysis and chiral Brønsted base catalysis proceeded with diastereocontrol, the latter approach offering higher levels of control than the former. However, copper catalysis enabled higher levels of control of enantioselectivity under the conditions tested. Considering the scalability of these two approaches, it is conceivable that the copper-catalyzed approach may require more stringent low-oxygen conditions to avoid catalyst oxidation and therefore may be more capricious; however, this is yet to be determined. Both the copper-catalyzed approach and the chiral Brønsted acid approach were developed using a 1 mol % catalyst; however, in both cases, the catalyst was still the key cost driver. As Michael acceptor **7** was used across each of the catalytic approaches investigated, optimization of its synthesis, avoiding the use of LiHMDS, was conducted. This work may be published separately at a later date.

In conclusion, we have disclosed our efforts optimizing three different catalytic asymmetric methods for setting the two nonadjacent stereocenters in a key building block for nirmatrelvir. Use of either Cu/FesulPhos or cyclopropenimine **11** resulted in high levels of enantiocontrol and moderate diastereocontrol, enabling multigram-scale preparation of **10**, a precursor to **3**.[8] These methods each avoid the use of cryogenic conditions and LiHMDS, which are limitations of the established chiral pool approach to this fragment.

EXPERIMENTAL PROCEDURES

(*S,S*)-10·(−)-CSA, Gram-Scale Asymmetric Michael Addition with Cu/FesulPhos Followed by Deprotection and (−)-CSA Salt Formation. Methyl 2-((diphenylmethylene)amino)acetate **5** (5.00 g, 19.7 mmol), *tert*-butyl 3-methylene-2-oxopyrrolidine-1-carboxylate **7** (95 weight% purity, 4.46 g, 21.5 mmol, ∼ 1.1 equiv), and anhydrous degassed IPA (50 mL, 10 mL g^{-1}) were charged into a 100 mL EasyMax vessel equipped with magnetic drive overhead stirring. The mixture was stirred at 20 °C until all the solids dissolved, then cooled to Tj = 0 °C (measured Tr = 1.3 °C), and then inerted with 3× vacuum/nitrogen cycles. In a nitrogen-filled glovebox, a suspension of $[Cu(MeCN)_4]PF_6$ (0.074 g, 0.20 mmol, 1 mol %) and (R_p)-FesulPhos (0.11 g, 0.23 mmol, ∼1.2 mol %) was prepared in anhydrous degassed IPA (15 mL, 3 mL g^{-1}). The yellow suspension was mixed with a vortex mixer for around 2 min, then transferred outside the glovebox in a vial with a septum cap, and then added to the EasyMax vessel via a wide bore syringe. The resulting yellow suspension was stirred for 10 min at Tj = 0 °C, and then DIPEA (8.53 mL, 48.9 mmol, ∼2.5 equiv) was added. Addition of DIPEA resulted in an orange solution. The reaction mixture was stirred at Tj = 0 °C for 20 h (monitoring via SFC method 1 showed the reaction reached completion after 14 h) before concentrating the mixture in vacuo. The thick orange oil was dissolved in 10 mL of THF, filtered through a silica plug, and washed with 500 mL of 1:1 EtOAc:heptane. The filtrate was concentrated in vacuo to give *tert*-butyl 3-(2-((diphenylmethylene)amino)-3-methoxy-3-oxopropyl)-2-oxopyrrolidine-1-carboxylate (*S,S*)-**9** as a yellow oil

https://doi.org/10.1021/acs.oprd.4c00109
Org. Process Res. Dev. 2024, 28, 2743−2754

(10.84 g, 2.95:1 DR, > 99% ee). Note that the DR by ^{1}H NMR was also 2.95:1. **LRMS** (ESI$^+$) calcd for $C_{26}H_{31}N_2O_5^+$ [M + H$^+$], 451.2; found, 451.2.

Methyl *tert*-butyl ether (TBME, 40 mL, 8 mL g^{-1}) at 40 °C was added to the crude Michael adduct, and the solution was transferred to a 100 mL EasyMax flask equipped with magnetic drive overhead stirring. L(−)-camphorsulfonic acid (9.28 g, 39.1 mmol) was charged, and the reaction mixture was refluxed for 16 h. Initially a gel formed, but this resolidified into off-white solids after ca. 20 min, coating the vessel walls. Acetone (70 mL, 14 mL g^{-1}) was added, and the reaction mixture was refluxed for 30 min. Addition of acetone suspended the solids. TBME (90 mL, 18 mL g^{-1}) was charged and the mixture was refluxed for 4 h before cooling to Tj = 0 °C at a ramp of 0.3 K min^{-1}. The product was isolated via filtration and washed with TBME:Acetone (2:1, 3 × 30 mL). The solids were transferred to a vacuum oven to dry overnight at 40 °C to afford the desired product (S)-1-methoxy-1-oxo-3-((S)-2-oxopyrrolidin-3-yl)propan-2-aminium((1*R*,4*S*)-7,7-dimethyl-2-oxobicyclo-[2.2.1]heptan-1-yl)methanesulfonate (*S,S*)-**10**·(−)-**CSA** (5.58 g, 67% yield, 99% weight purity by qNMR) as a free-flowing white powder. **^{1}H NMR** (400 MHz, methanol-d4) δ 8.03−7.18 (m, 0H), 4.25 (dd, *J* = 9.6, 3.6 Hz, 1H), 3.87 (s, 3H), 3.45−3.36 (m, 2H), 3.32 (d, *J* = 14.9 Hz, 1H), 2.88−2.75 (m, 2H), 2.75−2.63 (m, 1H), 2.44 (dddd, *J* = 12.2, 8.6, 5.2, 3.5 Hz, 1H), 2.36 (dt, *J* = 18.5, 4.2 Hz, 1H), 2.26 (ddd, *J* = 15.1, 4.6, 3.6 Hz, 1H), 2.07 (qt, *J* = 6.9, 3.6 Hz, 2H), 2.05−1.95 (m, 1H), 1.94−1.80 (m, 2H), 1.63 (ddd, *J* = 14.0, 9.6, 4.5 Hz, 1H), 1.49−1.37 (m, 1H), 1.15 (s, 3H), 0.88 (s, 3H). **^{13}C NMR** (101 MHz, methanol-d4) δ: 180.2, 169.3, 58.2, 52.45, 52.42, 48.2, 48.0, 47.8, 47.6, 47.4, 47.2, 47.0, 46.8, 42.7, 42.2, 40.7, 40.3, 31.6, 28.1, 26.4, 24.4, 19.1, 18.7. **HRMS** (ESI$^+$) calcd for $C_8H_{15}N_2O_3^+$ [M + H$^+$], 187.1077; found, 187.1075.

(*S,S*)-10·(−)-CSA, Gram-Scale Asymmetric Michael Addition Using Cyclopropenamine Catalyst 11, Followed by Deprotection and (−)-CSA Salt Formation. A 2 M solution of aq. NaOH (1.8 mL, 3.6 mmol) was added to a mixture of **11·HCl** (0.298 g, 0.512 mmol) in TBME (3 mL) at 20 °C, and the mixture was stirred for 10 min. The organic layer was separated, and the aqueous layer was extracted with TBME (2 mL). The combined organic layers were filtered over Na_2SO_4, and the filtrate was added directly to a mixture of pronucleophile **5** (7.06 g, 27.8 mmol, 1.1 equiv) and Michael acceptor **7** (5.00 g, 25.35 mmol, 1.0 equiv) in TBME (10 mL). The mixture was stirred at 35 °C for 4 h, and then (−)-CSA (11.77g, 50.7 mmol, 2 equiv) and water (0.46 mL, 1 equiv) were added. The mixture was then heated to 65 °C for 18 h, diluted with acetone (70 mL), refluxed for 20 min, diluted with TBME (130 mL), and then refluxed for an additional 4 h. The reaction was then cooled to 20 °C and filtered, and the solid was rinsed with a 2:1 mixture of TBME:acetone (3 × 30 mL). The solid was collected and dried under high vacuum to afford 7.2 g of (*S,S*)-**10**·(−)-**CSA** (66% yield) as an off-white solid. **^{1}H NMR** (600 MHz, methanol-d4) δ 4.23 (dd, *J* = 9.5, 2.7 Hz, 1H), 3.85 (s, 3H), 3.40−3.38 (m, 2H), 3.29 (s, 1H), 2.81−2.75 (m, 2H), 2.66 (dd, *J* = 20.4, 9.6 Hz, 1H), 2.44−2.39 (m, 1H), 2.36−2.32 (m, 1H), 2.24 (dt, *J* = 14.9, 3.8 Hz, 1H), 2.05−1.97 (m, 3H), 1.88 (dd, *J* = 20.4, 14.8 Hz, 2H), 1.61 (ddd, *J* = 13.3, 9.1, 4.0 Hz, 1H), 1.43−1.39 (m, 1H), 1.13 (s, 3H), 0.86 (s, 3H). **^{13}C NMR** (150 MHz, methanol-d4) δ: 218.3, 181.6, 170.7, 59.6, 53.8, 48.2, 44.0, 43.6, 42.0, 41.7, 32.9, 29.5, 27.8 (2C), 25.7 (2C), 20.4, 20.1. **HRMS** (ESI$^+$/QTOF) calcd for $C_8H_{15}N_2O_3$ [M$^+$], 187.1077; found 187.1073.

■ ASSOCIATED CONTENT

Supporting Information

The Supporting Information is available free of charge at https://pubs.acs.org/doi/10.1021/acs.oprd.4c00109.

Additional experimental procedures, ^{1}H and ^{13}C NMR spectra, chromatographs, and DSC spectra (PDF)

■ AUTHOR INFORMATION

Corresponding Authors

Robert Szpera − *Pfizer Worldwide Research and Development Discovery Park, Sandwich CT13 9NJ, U.K.*; orcid.org/0000-0003-1351-1750; Email: rob_szpera@hotmail.co.uk

Steven J. Fussell − *Pfizer Worldwide Research and Development Discovery Park, Sandwich CT13 9NJ, U.K.*; Email: steven.fussell@pfizer.com

Charles S. Shanahan − *Medicines for All Institute, Virginia Commonwealth University, Richmond, Virginia 23298, United States*; Email: charles.s.shanahan@haleon.com

Authors

Shanjun Huang − *Pfizer Worldwide Research and Development Discovery Park, Sandwich CT13 9NJ, U.K.*; orcid.org/0009-0006-0188-2545

Harriet A. M. Fenton − *Pfizer Worldwide Research and Development Discovery Park, Sandwich CT13 9NJ, U.K.*; orcid.org/0009-0001-3646-0055

William Waddington − *Pfizer Worldwide Research and Development Discovery Park, Sandwich CT13 9NJ, U.K.*

Adam E. S. Gymer − *Pfizer Worldwide Research and Development Discovery Park, Sandwich CT13 9NJ, U.K.*

Ian B. Moses − *Pfizer Worldwide Research and Development Discovery Park, Sandwich CT13 9NJ, U.K.*

Julia Buck − *Pfizer Worldwide Research and Development Discovery Park, Sandwich CT13 9NJ, U.K.*

Heather Ingram − *Pfizer Worldwide Research and Development Discovery Park, Sandwich CT13 9NJ, U.K.*

Robert Walton − *Pfizer Worldwide Research and Development Discovery Park, Sandwich CT13 9NJ, U.K.*

Sarah L. Aleshire − *Medicines for All Institute, Virginia Commonwealth University, Richmond, Virginia 23298, United States*

Juliana M. S. Robey − *Medicines for All Institute, Virginia Commonwealth University, Richmond, Virginia 23298, United States*

Hanuman P. Kalmode − *Medicines for All Institute, Virginia Commonwealth University, Richmond, Virginia 23298, United States*; orcid.org/0000-0002-1577-5103

Michel C. Nuckols − *Medicines for All Institute, Virginia Commonwealth University, Richmond, Virginia 23298, United States*

Nageswara R. Kalikinidi − *TCG GreenChem, Inc., Ewing, New Jersey 08628, United States*

Venumadhav Janganati − *TCG GreenChem, Inc., Ewing, New Jersey 08628, United States*

Sipak Joyasawal − *TCG GreenChem, Inc., Ewing, New Jersey 08628, United States*

Chanaka M. Amarasekarage − *TCG GreenChem, Inc., Ewing, New Jersey 08628, United States*

Chris H. Senanayake − *TCG GreenChem, Inc., Ewing, New Jersey 08628, United States*; orcid.org/0009-0009-3170-0687

B. Frank Gupton − *Medicines for All Institute, Virginia Commonwealth University, Richmond, Virginia 23298, United States;* orcid.org/0000-0002-8165-1088

Complete contact information is available at: https://pubs.acs.org/10.1021/acs.oprd.4c00109

Notes

The authors declare no competing financial interest.

■ ACKNOWLEDGMENTS

We acknowledge and thank IntelliSyn, who performed significant optimization on the chiral Brønsted base-catalyzed approach.

■ REFERENCES

(1) Lamb, Y. N. Nirmatrelvir Plus Ritonavir: First Approval. *Drugs* **2022**, *82* (5), 585−591.

(2) https://www.pfizer.com/news/press-release/press-release-detail/pfizer-receives-us-fda-emergency-use-authorization-novel.

(3) https://www.fda.gov/media/155050/download.

(4) Owen, D. R.; Allerton, C. M. N.; Anderson, A. S.; Aschenbrenner, L.; Avery, M.; Berritt, S.; Boras, B.; Cardin, R. D.; Carlo, A.; Coffman, K. J.; Dantonio, A.; Di, L.; Eng, H.; Ferre, R.; Gajiwala, K. S.; Gibson, S. A.; Greasley, S. E.; Hurst, B. L.; Kadar, E. P.; Kalgutkar, A. S.; Lee, J. C.; Lee, J.; Liu, W.; Mason, S. W.; Noell, S.; Novak, J. J.; Obach, R. S.; Ogilvie, K.; Patel, N. C.; Pettersson, M.; Rai, D. K.; Reese, M. R.; Sammons, M. F.; Sathish, J. G.; Singh, R. S. P.; Steppan, C. M.; Stewart, A. E.; Tuttle, J. B.; Updyke, L.; Verhoest, P. R.; Wei, L.; Yang, Q.; Zhu, Y. An oral SARS-CoV-2 M(pro) inhibitor clinical candidate for the treatment of COVID-19. *Science* **2021**, *374* (6575), 1586−1593.

(5) Owen, D. R.; Pettersson, M. Y.; Reese, M. R.; Sammons, M. F.; Tuttle, J. B.; Verhoest, P. R.; Wei, L.; Yang, Q.; Yang, X. Nitrile-containing antiviral compounds, Patent WO2021250648A1, 2021.

(6) Algera, R. F.; Allais, C.; Baldwin, A. F.; Becirovic, H.; Bowles, P.; Brown, A. R.; Buske, J. M.; Clarke, H. J.; Do, N. M.; Doyle, K.; Fifer, J.; Gray, K.; Happe, A.; Hardink, M.; Hubbell, A. K.; James, C.; Khadamkar, H. P.; Magano, J.; McInturff, E. L.; Mustakis, J.; Ozbuyukkaya, G.; Piper, J. L.; Place, D. W.; Ragan, J. A.; Rauschenberger, B.; Reyes, G.; Shehadeh, R.; Stanchina, C.; Stanley, M.; Weekly, R. M.; Weinstein, E.; Weisenburger, G. A.; Wood, E.; Yayla, H. G.; Yu, S. Synthesis of Nirmatrelvir: Development of an Efficient, Scalable Process to Generate the Western Fragment. *Org. Process Res. Dev.* **2023**, *27* (12), 2240−2249.

(7) Algera, R. F.; Allais, C.; Baldwin, A. F.; Busch, T.; Colombo, F.; Colombo, M.; Depretz, C.; Dumond, Y. R.; Faria Quintero, A. R.; Heredia, M.; Jung, J.; Lall, A.; Lee, T.; Liu, Y.; Mandelli, S.; Mantel, M.; Morris, R.; Mustakis, J.; Nguyen, B.; Pearson, R.; Piper, J. L.; Ragan, J. A.; Ruffin, B.; Talicska, C.; Tcyrulnikov, S.; Uyeda, C.; Weekly, R. M.; Zeng, M. Synthesis of Nirmatrelvir: Development of a Scalable Cobalt-Catalyzed Cyclopropanation for Manufacture of the Bicyclic [3.1.0]Proline-Building Block. *Org. Process Res. Dev.* **2023**, *27* (12), 2260−2270.

(8) Algera, R. F.; Allais, C.; Becirovic, H.; Brown, A. R.; Chen, B.; Clarke, H. J.; Concannon, P. E.; Du, Y.; Georgian, W.; Lee, J. W.; Lee, T.; Magano, J.; Perez Mandry, C.; Mehta, R.; Mull, E.; Pearson, R.; Peng, Z.; Piper, J. L.; Ragan, J. A.; Reyes, G.; Shen, H.; Ward, D. W.; Weekly, R. M.; Weisenburger, G. A.; Xu, P.; Yayla, H. G.; Zhang, M. Synthesis of Nirmatrelvir: Development of Magnesium Sulfate-Mediated Aminolysis for the Manufacture of the Eastern Fragment. *Org. Process Res. Dev.* **2023**, *27* (12), 2271−2279.

(9) Algera, R. F.; Baldwin, A. F.; Bowles, P.; Clarke, H. J.; Connor, C. G.; Cordi, E. M.; Do, N. M.; Nicholson, L. D.; Georgian, W.; Happe, A.; Herman, M. I.; Hilou, E.; James, C.; Johnson, A. M.; Kalinowski, M.; Kulkarni, S. A.; Launer-Felty, K. D.; Lee, J. W.; Lee, T.; Lopez, J.; McInturff, E. L.; Piper, J. L.; Place, D. W.; Ragan, J. A.; Rauschenberger, B.; Ryder, K.; Stanley, M.; Weisenburger, G. A.; Weekly, R. M.; Allais, C. Synthesis of Nirmatrelvir: Design and Optimization of an Efficient Telescoped Amidation−Dehydration Sequence. *Org. Process Res. Dev.* **2023**, *27* (12), 2250−2259.

(10) Hanessian, S.; Margarita, R. 1,3-Asymmetric induction in dianionic allylation reactions of amino acid derivatives-synthesis of functionally useful enantiopure glutamates, pipecolates and pyroglutamates. *Tetrahedron Lett.* **1998**, *39* (33), 5887−5890.

(11) Hanessian, S.; Schaum, R. 1,3-Asymmetric induction in enolate alkylation reactions of N-protected γ-amino acid derivatives. *Tetrahedron Lett.* **1997**, *38* (2), 163−166.

(12) Tian, Q.; Nayyar, N. K.; Babu, S.; Chen, L.; Tao, J.; Lee, S.; Tibbetts, A.; Moran, T.; Liou, J.; Guo, M.; Kennedy, T. P. An efficient synthesis of a key intermediate for the preparation of the rhinovirus protease inhibitor AG7088 via asymmetric dianionic cyanomethylation of N-Boc-l-(+)-glutamic acid dimethyl ester. *Tetrahedron Lett.* **2001**, *42* (39), 6807−6809.

(13) Vuong, W.; Vederas, J. C. Improved Synthesis of a Cyclic Glutamine Analogue Used in Antiviral Agents Targeting 3C and 3CL Proteases Including SARS-CoV-2 M(pro). *J. Org. Chem.* **2021**, *86* (18), 13104−13110.

(14) Qin, H.; Jin, C.; Odilov, A.; Mintah Bonku, E.; Zhu, F.; Liu, Q.; Shen, J.; Aisa, H. A. Optimized Synthesis of a Key Intermediate of Nirmatrelvir. *Org. Process Res. Dev.* **2023**, *27* (1), 78−83.

(15) This content is a preprint and has not been peer-reviewed. Szpera, R.; Huang, S.; Fenton, H. A. M.; Waddington, W.; Gymer, A. E. S.; Moses, I.; Buck, J.; Ingram, H.; Fussell, S. J.; Walton, R.; Shanahan, C. S.; Aleshire, S. L.; Robey, J. M. S.; Kalmode, H. P.; Nuckols, M. C.; Kalikinidi, N. R.; Janganati, V.; Joyasawal, S.; Amarasekarage, C. M.; Senanayake, C.; Gupton, B. F. Development of New Catalytic Asymmetric Routes towards a Cost-Driving Building Block of Nirmatrelvir. *ChemRxiv* **2024**, DOI: 10.26434/chemrxiv-2024-51d8j.

(16) Strohmeier, M.; Leach, K.; Zajac, M. A. Asymmetric conjugate addition of glycine derivatives under copper catalysis. *Angew. Chem., Int. Ed. Engl.* **2011**, *50* (51), 12335−12338.

(17) Liu, B.; Zhang, Z.-M.; Xu, B.; Xu, S.; Wu, H.-H.; Liu, Y.; Zhang, J. Cu(i)-catalyzed Michael addition of ketiminoesters to β-trifluoromethyl β,β-disubstituted enones: rapid access to 1-pyrrolines bearing a quaternary all-carbon stereocenter. *Org. Chem. Front.* **2017**, *4* (9), 1772−1776.

(18) Hernandez-Toribio, J.; Arrayas, R. G.; Carretero, J. C. Enantiocontrolled synthesis of beta-branched alpha-amino acids by using Cu(I)-catalyzed 1,4-addition of glycine imines to beta-substituted gem-diactivated olefins. *Chemistry* **2011**, *17* (23), 6334−6337.

(19) Konno, T.; Watanabe, S.; Takahashi, T.; Tokoro, Y.; Fukuzawa, S. Silver/ThioClickFerrophos complex as an effective catalyst for asymmetric conjugate addition of glycine imino ester to unsaturated malonates and alpha-enones. *Org. Lett.* **2013**, *15* (17), 4418−4421.

(20) Tsubogo, T.; Saito, S.; Seki, K.; Yamashita, Y.; Kobayashi, S. Development of catalytic asymmetric 1,4-addition and [3 + 2] cycloaddition reactions using chiral calcium complexes. *J. Am. Chem. Soc.* **2008**, *130* (40), 13321−13332.

(21) Kobayashi, S.; Tsubogo, T.; Saito, S.; Yamashita, Y. Calcium-catalyzed diastereo- and enantioselective 1,4-addition of glycine derivatives to alpha,beta-unsaturated esters. *Org. Lett.* **2008**, *10* (5), 807−809.

(22) Hut'ka, M.; Tsubogo, T.; Kobayashi, S. Synthesis of Glutamic Acid and Highly Functionalized Pyrrolidine Derivatives by Utilizing Tunable Calcium Catalysts for Chemoselective Asymmetric 1,4-Addition and [3 + 2] Cycloaddition Reactions. *Adv. Synth. Catal.* **2013**, *355* (8), 1561−1569.

(23) Cabrera, S.; Gomez Arrayas, R.; Carretero, J. C. Highly enantioselective copper(I)-fesulphos-catalyzed 1,3-dipolar cycloaddition of azomethine ylides. *J. Am. Chem. Soc.* **2005**, *127* (47), 16394−16395.

(24) Llamas, T.; Arrayás, R. G.; Carretero, J. C. Catalytic Enantioselective 1,3-Dipolar Cycloaddition of Azomethine Ylides with Vinyl Sulfones. *Org. Lett.* **2006**, *8* (9), 1795−1798.

(25) Yildirim, O.; Grigalunas, M.; Brieger, L.; Strohmann, C.; Antonchick, A. P.; Waldmann, H. Dynamic Catalytic Highly Enantioselective 1,3-Dipolar Cycloadditions. *Angew. Chem., Int. Ed. Engl.* **2021**, *60* (36), 20012−20020.
(26) Stoessel, F. *Thermal Safety of Chemical Processes*. 2008.
(27) Bandar, J. S.; Barthelme, A.; Mazori, A. Y.; Lambert, T. H. Structure−activity relationship studies of cyclopropenimines as enantioselective Brønsted base catalysts. *Chem. Sci.* **2015**, *6* (2), 1537−1547.
(28) -5. Bandar, J. S.; Lambert, T. H. Enantioselective Bronsted base catalysis with chiral cyclopropenimines. *J. Am. Chem. Soc.* **2012**, *134* (12), 5552.
(29) Ballini, R.; Palmieri, A.; Petrini, M. Catalysts' evolution in the asymmetric conjugate addition of nitroalkanes to electron-poor alkenes. *Org. Chem. Front.* **2022**, *9* (21), 6077−6113.
(30) Quintavalla, A.; Lanza, F.; Montroni, E.; Lombardo, M.; Trombini, C. Organocatalytic conjugate addition of nitroalkanes to 3-ylidene oxindoles: a stereocontrolled diversity oriented route to oxindole derivatives. *J. Org. Chem.* **2013**, *78* (23), 12049−12064.
(31) Manzano, R.; Andres, J. M.; Alvarez, R.; Muruzabal, M. D.; de Lera, A. R.; Pedrosa, R. Enantioselective conjugate addition of nitro compounds to alpha,beta-unsaturated ketones: an experimental and computational study. *Chemistry* **2011**, *17* (21), 5931−5938.
(32) Maule, I.; Razzetti, G.; Restelli, A.; Palmieri, A.; Colombo, C.; Ballini, R. Thermal Stability Evaluation of Nitroalkanes with Differential Scanning Calorimetry. *Org. Process Res. Dev.* **2021**, *25* (4), 781−788.

https://doi.org/10.1021/acs.oprd.4c00109
Org. Process Res. Dev. 2024, 28, 2743−2754